Environ Earth Sci (2011) 62:883–896
DOI 10.1007/s12665-010-0575-6

ORIGINAL ARTICLE

Geotechnical characterization and facies change detection of the Bogacay coastal plain (Antalya, Turkey) soils

Nihat Dipova

Received: 13 December 2008 / Accepted: 28 April 2010 / Published online: 20 May 2010

Abstract The Bogacay Plain is well known tourist site in Turkey, which is famous for its wide beaches. However, almost 60% of the area is now occupied by buildings, and some of the high-rise buildings suffer from foundation settlement and tilting. Soils of the plain are of lagoonal origin; all of the facies which are typical of the lagoonal environment are present in the geological profile. Because of variation in grain size and development of a weathered crust, the fine-grained soils of the central-lagoon environment are highly variable with regard to their engineering properties. The compression indices of clays range from 0.25 to 0.55 and correlate relatively well with initial void ratio, liquid limit, and moisture content. Over consolidation ratio varies between 1.4 and 10 and decreases from the surface down to the base of the weathered-crust zone. The undrained shear strength of clays decreases with depth for the first 6 m; this behaviour is because of apparent over-consolidation in the weathered-crust zone. Sedimentary facies and their boundaries can be detected using CPT data; moreover, for profiling and facies-boundary detection, SPT and seismic sounding are not as effective as CPT.

Keywords Characterization · Clay · CPT · Facies · Lagoonal soils

Introduction

Sedimentary environments in coastal lagoons are of mainly three types: barrier, bay-head delta, and central basin (Reinson 1992). Barrier environments are a distinctive component of coastal plains subjected to high wave energy; their sediments comprise well-sorted coarse sand or gravel. Sediments of the bay-head delta environment are sand and gravel. Fluvial channels transect the central basin of the lagoon. Central-basin environments constitute the deeper, quieter parts of the lagoon; thus, their sediment types range from clay to fine sands. Bivalve shells are widespread and concentrations of organic material are generally high, giving a dark grey appearance to the sediment. In the event of sea-level highstands, sand flats and mudflats may be deposited. Peat, on the other hand, develops where water depth is shallow. In such a depositional environment, soil layers are not always horizontal and the soil profile may change even within a centimetre.

Bogacay coastal plain of lagoon origin, which is located southwest of the city of Antalya, is the subject of this study (Fig. 1). The study area is a well-known tourist site of Antalya which is famous with its wide beaches. In addition to touristic activities, Antalya Harbour and Antalya Free Trade Zone are located in the south-west margin of the beach. Such attractive features of the study area, rapidly increasing population of Antalya, and scenic beauty of the Mediterranean cost, have increased the value of the land of Bogacay Plain. Former orange fields and former peaty and marshy areas, which were dried by canals, became land parcels and high-rise buildings started to be constructed after the 1990s. A residential and commercial city development plan was prepared for an area of about 13 km^2 at the south part of the plain. The north part (42 km^2) will be the second stage of this plan. Elevation of the south part is 2–9 m above msl (mean elevation is 5 m). The north part starts from 9 m and continues up to 40 m above msl. At the end of 1995, in the south, approximately 20% of the area was occupied by buildings. At the end of 2008 this ratio is

N. Dipova (✉)
Department of Civil Engineering, Akdeniz University, Dumlupinar Bulvari, Kampus, 07058 Antalya, Turkey
e-mail: ndipova@akdeniz.edu.tr

about 60%. However, some of these luxurious, comfortable, and rather expensive high-rise buildings suffer from foundation instability. Cracking and fissuration of the walls and overall tiltings are typical indications of the foundation problem from which the buildings are suffering. Some are still unstable and unused and some have been repaired by underpinning techniques.

The objective of this study was to elucidate the soil conditions of the Bogacay Plain for better understanding the causes of the instability problems of area structures and for planning future engineering works. Thus, this study is focussed on determination of geological profile, sedimentary facies, and the index and mechanical properties of the soils. The settlement problems of foundations and the relationship between sedimentary facies and geotechnical data are also discussed.

Geology of the Antalya region

Antalya is located at the southern margin of the Western Tauride Belt. The main rock units of the region are divided

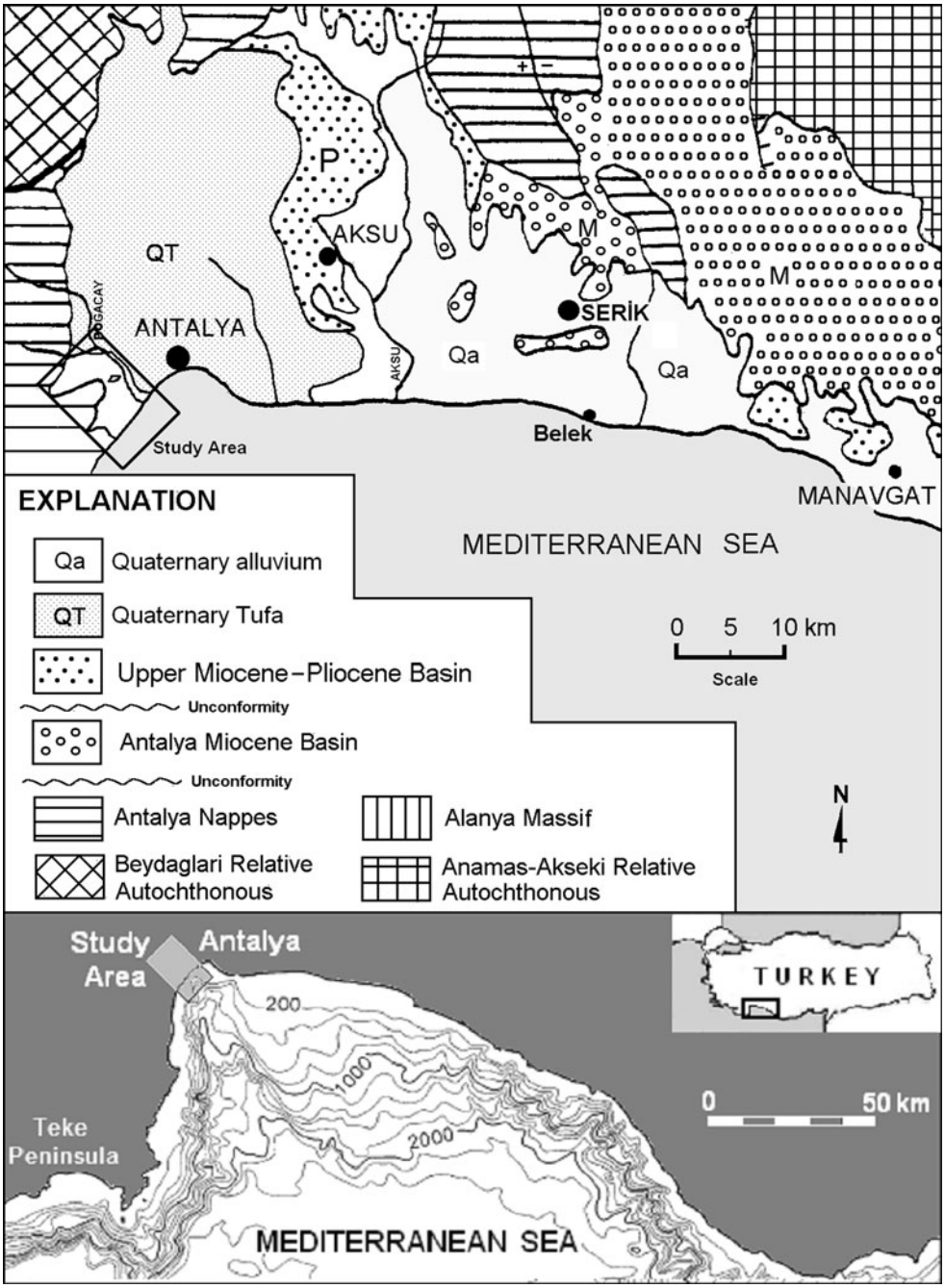

Fig. 1 Regional geological setting (after Akay et al. 1985)

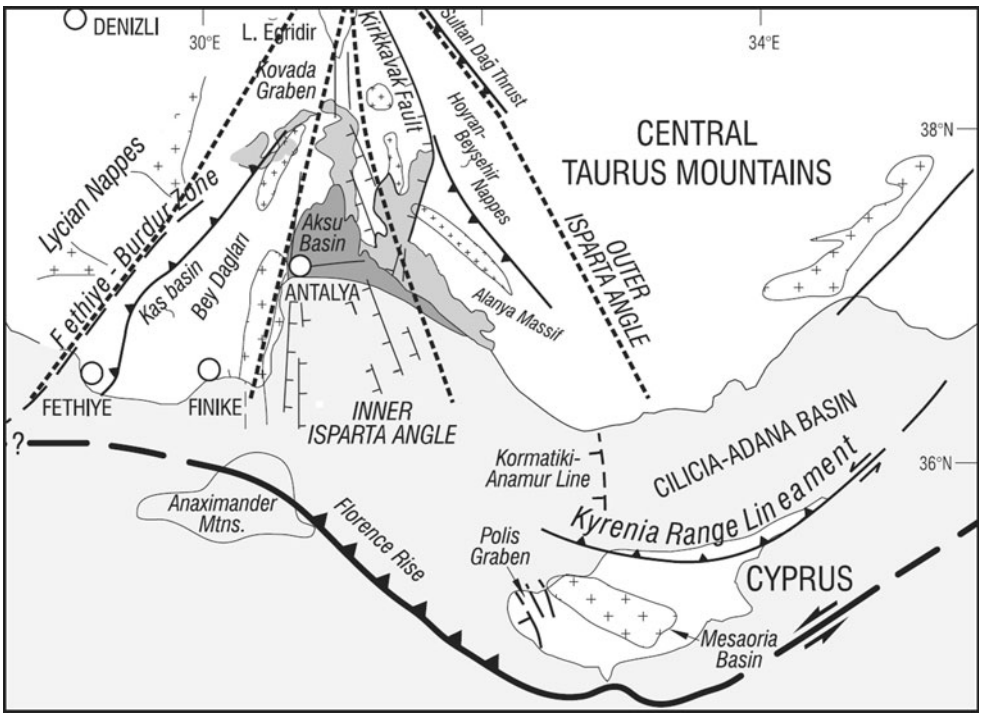

Fig. 2 Main neotectonic lineaments and structural units in the region (after Glover and Robertson 1998b)

into allochthonous and autochthonous units (Fig. 1). One of the main autochthonous units is the Anamas–Akseki (relative autochthonous); this unit consists of platform-type carbonate sediments that were deposited between the Late Cambrian and Eocene. Another autochthonous unit is the Beydaglari (relative autochthonous), comprising platform-type carbonate sediments of Jurassic to Miocene age (Akay et al. 1985). Together, these two units comprise the basement on to which the allochthonous units were emplaced and younger autochthonous units were deposited conformably.

The younger autochthonous units are divided into two groups. The first group comprises sediments deposited in the Antalya Miocene basin. The basin contains sandstone, conglomerate, limestone, clayey limestone, brecciated limestone, claystone and shale. The basin opened during the Oligocene and closed in the Late Miocene. The second basin is an Upper Miocene–Pliocene basin located west and south of the Aksu River. The basin opened in the Messinian and closed in the Early Pliocene, and contains conglomerate, sandstone, limestone, and calcareous claystone (Akay et al. 1985). The youngest autochthonous unit of the area is the Antalya tufa (Plio-Quaternary), which extends from the Aksu River in the east, to the Antalya Nappes in the west, and to the Beydaglari in the north. The Antalya tufa unconformably overlies Miocene deposits to the east and a Cretaceous ophiolitic complex to the west. Below the tufa layer, the nature of the contact between the Miocene deposits and the ophiolitic complex is unclear.

The main allochthonous unit of the area is the Antalya Nappes, comprising mainly marine sediments deposited in the basin between the Beydaglari unit and the Anamas–Akseki unit. After deposition was completed, the Antalya Nappes were thrust over the Beydaglari and Anamas–Akseki units. In the study area the Antalya Nappes are represented by Cretaceous limestones and ophiolitic sequences. The Bogacay Plain evolved during the Quaternary, on an embayment opened between the Antalya Nappes and the Antalya tufa.

The study area is located in an active tectonic region. Both Senel (1997) and Glover and Robertson (1998a) explain the Aksu Plain, in which the study area is located, by means of block faulting that resulted from an extensional regime. The study area is thought to have been affected by three well-documented active fault systems: the Fethiye–Burdur Zone, the Aksu Fault, and the Antalya Bay fault (Fig. 2). Within a 100-km radius of the study area, during the years 1900–2005, 338 earthquakes ($M = 4.2$–6.1) have been recorded.

Evolution of the Bogacay coastal plain

Pre-Holocene evolution of the southwest Anatolia was explained by Glover and Robertson (1998a). According to this model; westward movement of the Anatolian block has produced a tensional regime in western Anatolia and the uplift of central Anatolia. This mechanism is expressed in the vicinity of Antalya via opening of the Aksu Basin as a

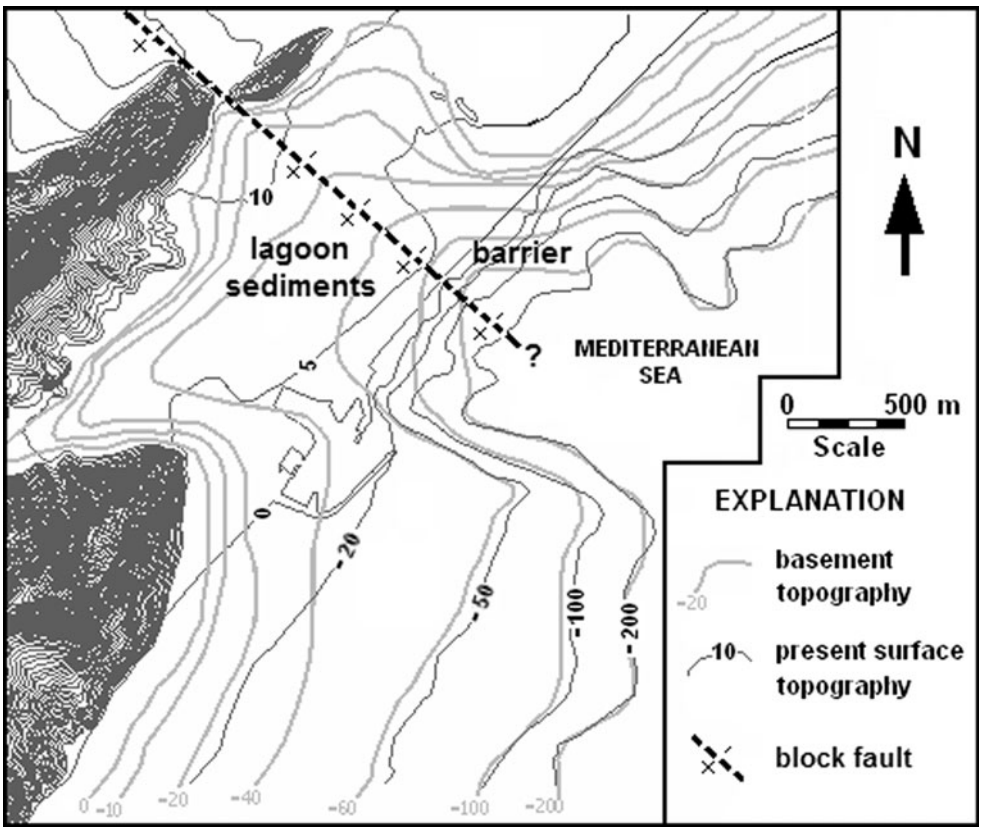

Fig. 3 Pre-Holocene basement topography of the study area

half-graben, thus producing down-drop of the western part and uplift of the eastern part. Another important factor is sea-level changes. According to previous workers (Kelletat 2005; Kayan 1988), the sea level fell about 100 m in south-east Anatolia during the last glacial maximum and increased to its current level during the Holocene.

Evolution of the Bogacay Plain was closely related to eustatic sea-level changes and tectonic activity. Following the very rapid sea-level rise that occurred between 18 and 6 ky BP, former valleys and embayments turned into bays in the west of Antalya (Teke Peninsula). However in the east, because of continental uplift, the relative sea-level rise was less than in the west. The ruins of ancient cities (Faselis and Kekova; 2,000–2,500 years BP), located to the west, are submerged 2–3 m below sea level. However Aspendos, which is located 50 km east of the study area, once a river-mouth harbour city at sea level, is now 15 m above sea level.

Deposition of the Antalya tufa was also related to the mechanism described above. At the western margin of the half-graben, fan deltas are typical in front of the fault. A continuation of the block fault is thought to be exposed at Hurma (Bogacay Plain) (Fig. 3). The fault may be responsible for the elevation difference between Domuzburnu Hill and Kucukdag Hill, creating a deep valley. Today, this valley is covered by lagoonal and alluvial sediments; however, the valley extends undersea in front of a lagoon barrier.

By evaluation of borehole logs of this study, geophysical data of DSI (1977), bathymetric map, and undersea seismic data of Tezcan and Okyar (2006), the pre-Holocene basement morphology was reconstructed (Fig. 3). The thickness of these sediments is generally less than 50 m, and the mean value is 40 m, except in front of the valley located in the central part of the plain, where the thickness reaches to 75 m. The bathymetric map and seismic data suggest that the shelf in front of the plain terminates with a steep slope on its seaward side. This slope is probably controlled by the seaward continuation of normal faults that developed along the graben structure.

The current geological map of the area is shown in Fig. 3. Borehole data (borehole locations are shown in Fig. 4a) show that Quaternary sediments overlie ophiolitic mélange in the west and tufa in the east (Fig. 4b). Beneath the tufa, the ophiolitic mélange extends down to borehole depth. Before the sea-level rise, the pre-existing topography was a deep valley eroded into ophiolitic rocks. A present-day bathymetry map shows that the valley extends to the south below −100 m. To the north, the valley extends to the intersection of the Domuzburnu and Kucukdag hills. Thus, these two hills may have been separated because of a fault plane, or erosion, or both. The

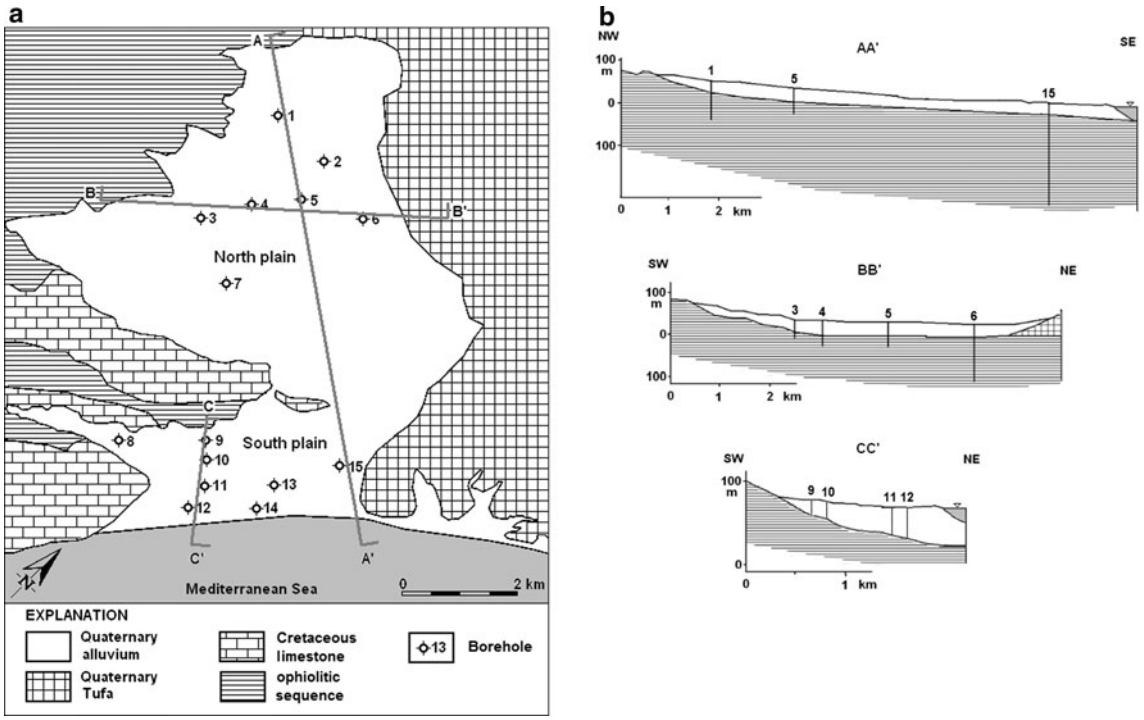

Fig. 4 **a** Geological map and **b** geological cross-sections

difference in elevation and the lateral offset between the hills supports the oblique-fault hypothesis.

Following the sea-level rise, the valley was inundated and the area became a bay. Granular material carried by Bogacay stream was deposited in front of the bay by sea currents and began to form a barrier beach. When the barrier beach sealed off the entire bay, the area became a lagoon that is fed partly by the Bogacay River and groundwater, and partly by drainage through the Sarısu inlet. In the low-velocity environment of the central lagoon, fine-grained material (silt and clay) settled and, because the lagoon was fed from the north, a bay-head delta formed at Hurma (in front of the intersection of the two hills) and shallow-water peat developed.

Borehole data show that in the central part of the plain, the dominant soil unit is blue–green silty clay, a material typical of a lagoonal environment. However, 4–6 m below sea level, a sand layer is present within the lagoonal mud. The thickness of the sand unit and the grain size of the sand varies laterally; in some localities the sand is replaced by peat. This sand layer is overlain by a soft mud containing bivalve shells. When sea level was static, because of a combination of tidal effects and floods, sand flats and mudflats were deposited. After sea level had risen sufficiently, deposition of lagoonal mud (silt–clay) continued; this situation is also typical of other coastal-plain areas of the Teke Peninsula. In the deposits of the Esen and Finike plains, 4–5 m below the current sea level, sand and peat layers were interpreted by Oner (1995) as representative of a static sea-level stand 4,220 years BP.

After closure of the lagoon, the current elevation of the coastal plain is approximately 5 m above sea level. The mean groundwater level is at 1.8 m. Below the land surface down to −4 m, the colour, texture and physical properties of the deposits differ from those farther below. Even though their origins are the same, oxidation, leaching, temperature, and groundwater fluctuations resulted in chemical and mineralogical changes that led to crust formation.

On the basis of grain size, texture, colour, and elevation, eight different lithofacies within the Holocene sediments were identified from borehole samples. The data set consists of 30 continuously cored boreholes with depths of 10–5 m. The cross-section in Fig. 5 illustrates the distribution of the facies.From older to younger, the lithofacies may be described as follows.

Barrier beach (BB)

This facies comprises coarse sand with varying amounts of gravel and beachrock. The dominant grain size is 1–8 mm and the fines (silt–clay) content is less than 5%. In some layers, the silt content is higher and, in particular—at about 6–8 m depth—the predominant grain size is fine sand and the silt content is above 10%. No organic material was detected in the boreholes. The barrier-beach facies comprises limestone, chert, and serpentinite. Grains are

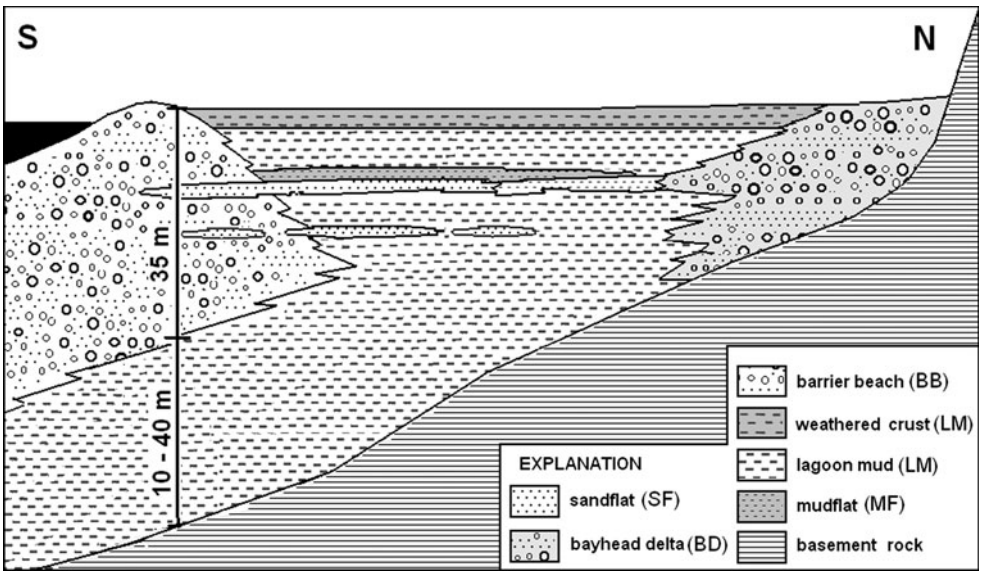

Fig. 5 Geological cross-section along the deepest part of the valley (not to scale)

well-rounded but not spherical; in particular, gravel-size particles are ellipsoidal. The maximum elevation of the barrier is 7 m above sea level. The maximum thickness of this facies was measured as 35 m.

From the surface downward, cemented sand and gravel layers have been detected at various depths and concluded to be beachrock. Although there has been a major debate concerning the origin of beachrock, this rock type typically forms within the vadose zone in which meniscus cements are produced at grain contacts. There are, however, some general conditions for the formation of beachrock (Kneale and Viles 2000); for example, warm water supersaturated with $CaCO_3$, high water flux at the sediment–water interface, good permeability of surface sediments, and a stable substrate combined with a slow sedimentation rate. DSI (1977) reported a high-calcium groundwater discharge to the sea (5.5×10^6 m^3/year). Moreover, the Mediterranean climate and grain properties support the designation of these cemented sands and gravels as beachrock.

Fluvial alluvium (A)

River-bed deposits and other fluvial deposits which have been deposited in old river beds were grouped into this facies. This facies is the coarsest of the all the facies and comprises coarse gravels and medium to fine sands. The sources of the materials of this facies were Cretaceous limestone and ophiolitic mélange.

Sand flat (SF)

This facies is composed of light grey to brownish-yellow, fine-grained, well-sorted sands. Intercalated mud layers also occur throughout this facies. Mean sediment size is between 0.5 and 2.0 mm. Whole shells or large shell fragments are widespread. The most typical sedimentary structures are parallel, horizontal laminations. This facies, with a maximum thickness of 1 m, is present in most cores from the back-barrier plain 8–10 m below the surface. Although of varying thickness, the sand-flat facies is widespread in the area. This kind of deposition is typical of tidal deltas and tidal-flat areas. However, the Mediterranean Sea is a closed sea and tidal oscillation is relatively limited. Thus, the sand layers may have formed by scattering of beach and delta sand by microtidal energy.

Mudflat (MF)

This facies consists of more than 95% fines, has significant bivalve-fossil content, and overlies the sand-flat facies along a gradational contact. The average upper and basal elevations of this facies are 6 and 8 m, respectively, the maximum thickness is 2.5 m, and the colour of the sediment varies from light to dark grey. This facies should be the uppermost sedimentary unit throughout the back-barrier plain, representing an historical sea-level highstand.

Bay-head delta (BD)

The northern part of the plain comprises a bay-head delta. This unit appears as a fan having a 400-m radius, which radiates from between two hills. Because continuous coring in delta deposits could not be achieved, coarsening upward sequences typical of bay head deltas were not detected. This facies represents a lagoon entrance, and flooding in the rainy season resulted in deposition of laminated, gravelly and sandy mud with local lenses of pure sand and gravel.

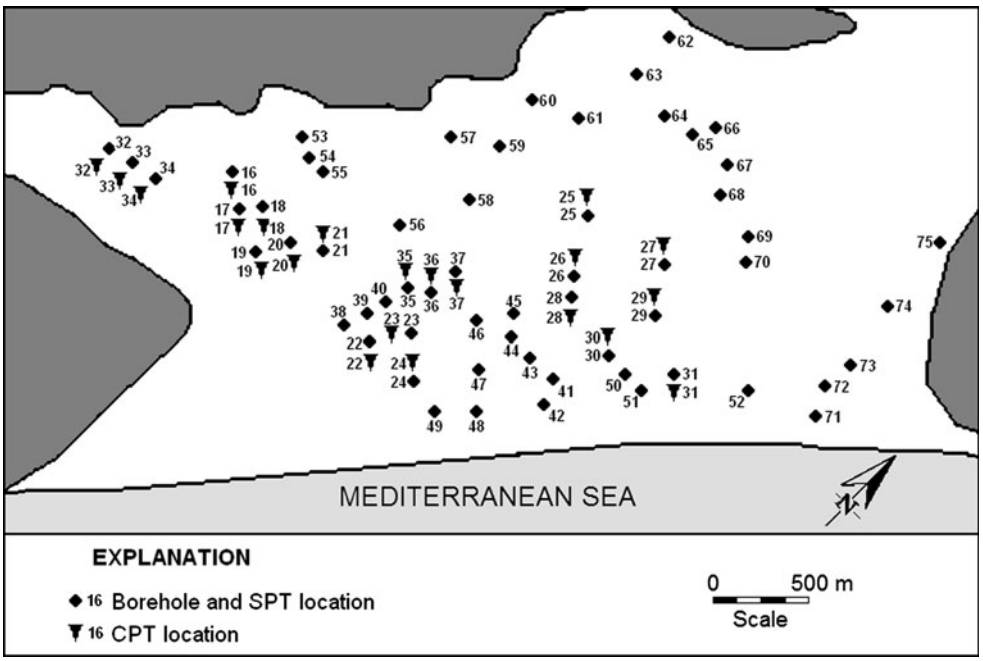

Fig. 6 Borehole and in-situ test locations

Lagoon mud (LM)

This facies comprises blue–grey mud with, generally, 10% sand, 40% silt, and 50% clay, and contains abundant brackish-marine faunal remains; bivalve and gastropod fossils are widespread in the deposits. The mud deposits are rich in plant roots with local peat layers. Weathered clay crust (WCC) is the uppermost part of the lagoon mud (LM) facies. The obvious differences arise from post-depositional processes. Emergence due to relative sea-level changes and groundwater-level fluctuations resulted in chemical weathering. Furthermore, leaching occurred because of surface runoff. Desiccation cracks increased the intensity of weathering and leaching. These changes resulted in reduced void ratio and increased strength. The thickness of this crust in the Bogacay Plain varies from 3.5 to 5.5 m. Clays of this part are brownish-grey and of silt–clay character. Mud cracks are abundant, and these features indicate exposure to air.

Geotechnical properties of soil units

Determination of soil properties is important for construction of engineering–geological models and geotechnical design. Moreover, it has been recognised that the geomechanical properties of soil are strongly affected by the conditions of the depositional environments. Thus, in addition to determining the engineering properties of the soils, identifying depositional environments was also an objective of this study. Geotechnically speaking, mud layers representing the central lagoon are the most interesting units, and more attention was paid to these soils. Index, strength, and deformability properties of the silty and clayey soils were determined, and are discussed in detail.

Boreholes and standard penetration tests (SPT)

Geotechnical data from 75 boreholes, ranging from 10 to 100 m in depth, were evaluated to elucidate the geological

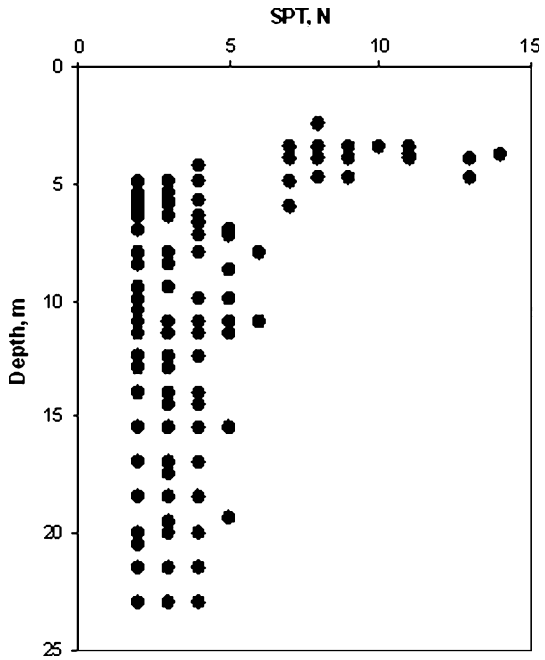

Fig. 7 Variation of SPT with depth

profiles of the study area (Fig. 6). In order to perform thorough evaluation and testing, a detailed drilling program was conducted and 20 boreholes of 10–30 m depth were drilled. During the boring of these holes, the standard penetration test (SPT) was done with a split spoon sampler and safety hammer. The sampler is driven into the soil to a depth of 450 mm by means of a 63.5 kg hammer free-falling 760 mm with each blow. SPT test results are given in Fig. 7.

Because drilling technique and sample quality are important in the reliable determination of soil properties, special attention was paid to drilling and sampling. Boreholes were drilled using 90 mm augers without using a water flush. Each manoeuvre was only 50 cm, and continuous core sampling or in situ testing were carried out without leaving a blank zone. Undisturbed core samples were used for visual inspection and geotechnical testing.

Cone penetration testing (CPT)

In this study, mechanical (Gouda Dutch cone penetrometer) and CPTU electrical cone penetration tests (piezocone) were carried out at 22 sites, following American society for

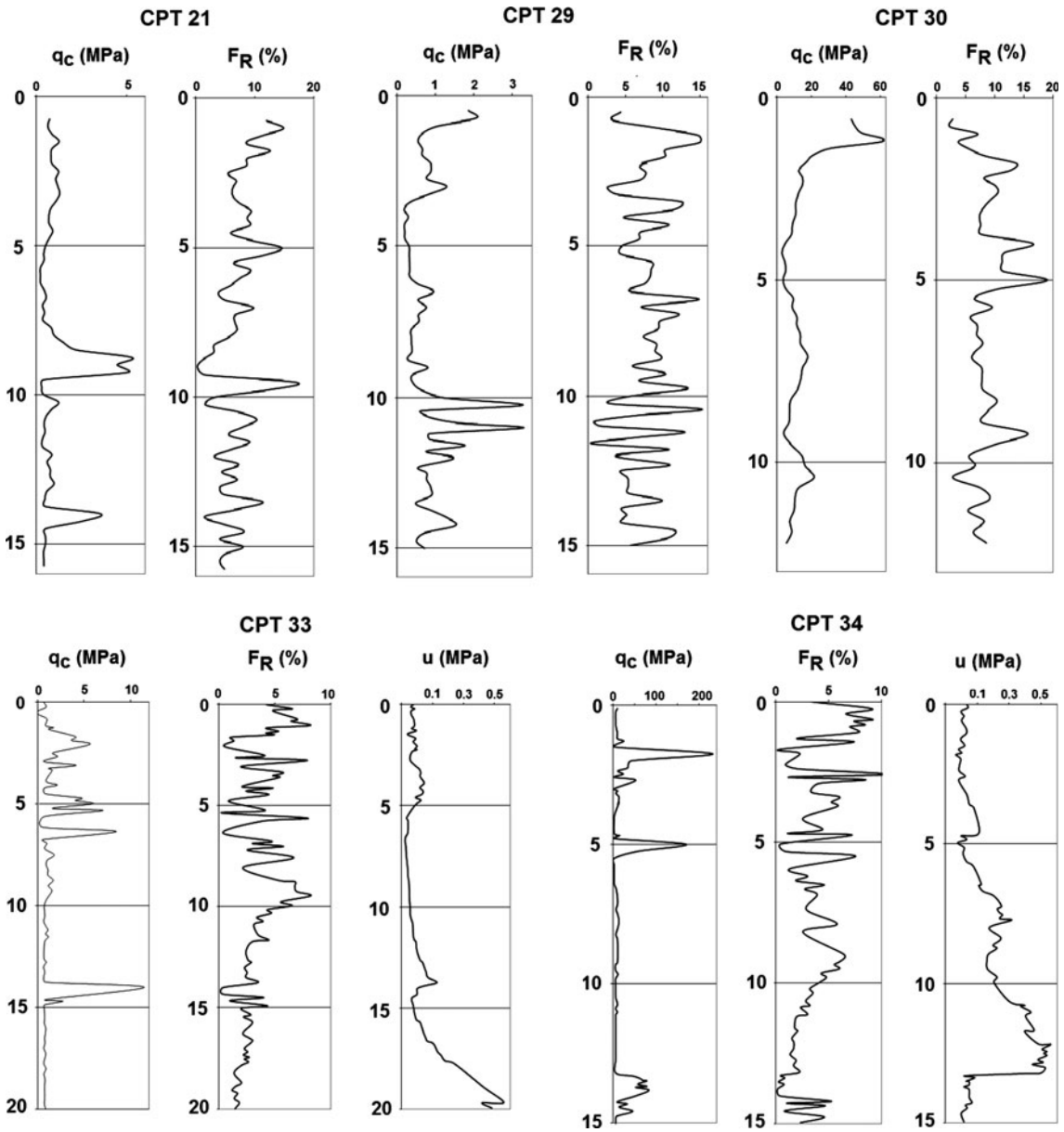

Fig. 8 Characteristic CPT test results

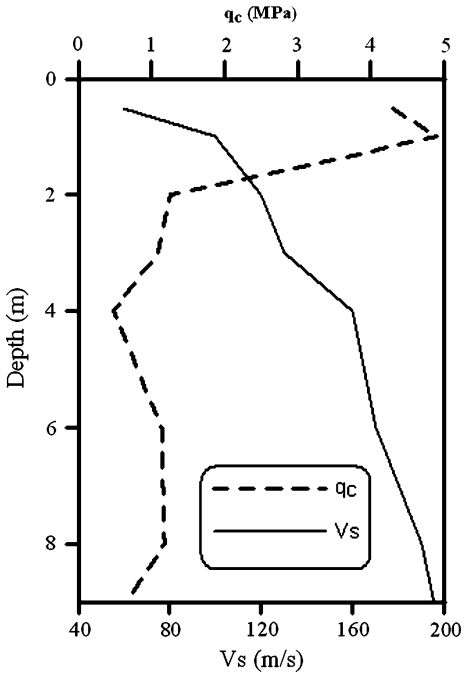

Fig. 9 Variation of V_s with depth and comparison with q_c

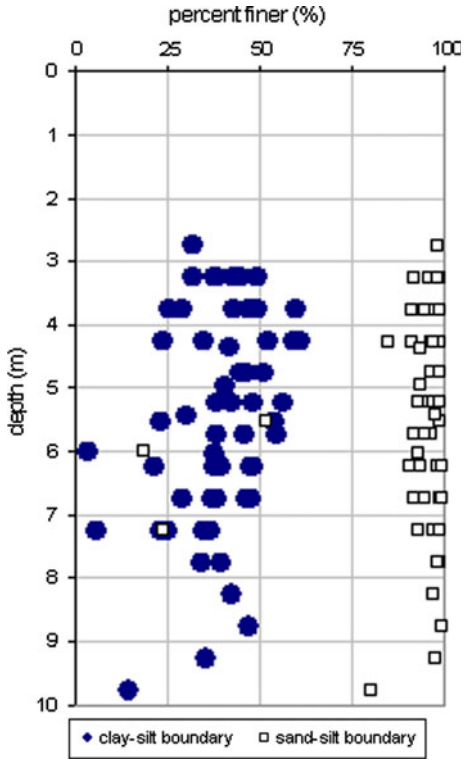

Fig. 10 Particle-size variation of soils with depth

testing and materials (ASTM) procedures, and evaluated. At each location, a CPT probe penetrated to a depth of 10–30 m. The diameter of the cone was 35.7 mm and the tip angle 60° with a 150 cm^2 friction sleeve. The speed of penetration was 2 cm/s. CPT tests were made at borehole locations in order to make observations and correlations. Characteristic CPT logs are shown in Fig. 8.

Geophysical Investigations

In this study, geophysical investigations—including electrical resistivity and seismic refraction—were carried out. Most of the resistivity tests evaluated in this study were done by DSI (1977) for groundwater-investigation purposes; these included measurements at 35 different locations which were 500–1,000 m apart and taken down to a maximum depth of 200 m. As a result of these measurements, the basement topography and geological properties of the cover soils were determined.

Seismic-refraction tests were carried out at 11 different locations, and V_p and V_s values were determined using forward and reverse-travel techniques. The layer thicknesses of the profiles were calculated by the delay-time method. Because the groundwater table is close to the surface, and because of obstacles on the roll-out line, maximum penetration depth was limited to 12 m. Measured V_s values are dependent on soil depth (Hamilton 1976; Holzer et al. 2005). Even in the weathered-crust zone, wherein density and strength decrease with depth, results show that V_s values increase with depth (Fig. 9).

Index properties of soils

Grain-size distribution, Atterberg limits and densities were determined according to ASTM standards. Index properties of soil samples are dependent on depositional environments (facies). The plasticity index of the lagoonal-mud facies varies from 20 to 45% and most of the lagoonal muds are of the CH type, with average liquid limits of 55. The average water content is between 30 and 40%. The liquid limit of the mudflat facies rises to an average value of 60%. Sieve-analysis results for samples below groundwater down to 10 m depth are given in Fig. 10.

In a recent study (Uzer 2006), the clay mineralogy of the Bogacay Plain was investigated by means of X-ray diffractometry (XRD) on samples collected from the surface to depths of 22.5 m, in the southern part of the plain. The samples were found to be composed of kaolinite, smectite, chlorite and illite. XRD results show high peaks for quartz, calcite, and feldspars; these are all believed to be silt-size particles, however. As can be seen in Fig. 11, regardless of sand layers, the mineralogy seems to be quite consistent over the entire depth. A substantial change appears in the weathered-crust unit—at depths down to −3 m, and below −12 m. In the central part of the profile, clay mineralogy was determined as 45% smectite, 28% kaolinite, 17% illite, and 10% chlorite.

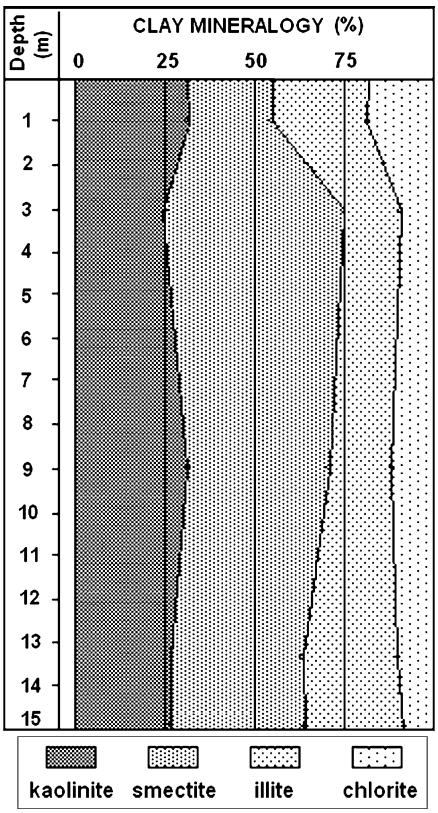

Fig. 11 Mineralogy of clayey soils (Uzer 2006)

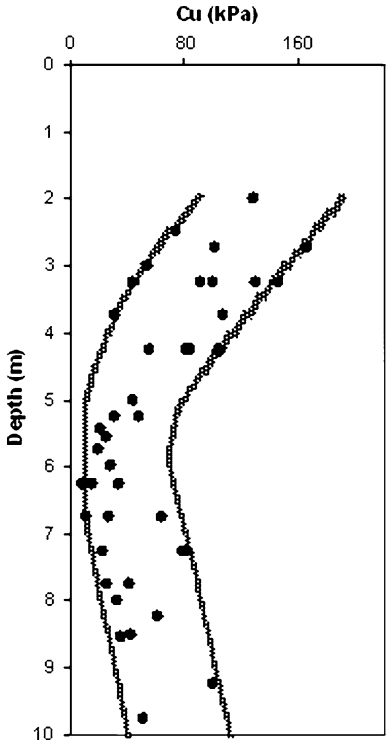

Fig. 12 Variation of Su with depth

Undrained shear strength of silty clays

Unconfined compression and undrained-unconsolidated (UU) tests were carried out following ASTM procedures. The diameters and heights of the specimens were 38 and 76 mm, respectively. However the results of the laboratory tests are usually subject to uncertainties, because of the inevitable sample disturbance. In this work, the conventional UU test method was chosen to determine undrained shear strength. Because the triaxial UU test is quick and easy it is a common test method, and comparison with other databases is possible. Because of sample heterogeneity and difficulties in obtaining samples, the multi-stage test method was preferred. In this method, axial load was applied under constant cell pressure until the specimen failed; the cell pressure was then raised and axial loading continued to obtain a new peak deviator stress. Test results show low internal-friction angles (<6, with an average of 3). These low internal-friction angles for undrained loading are because of the silty character of the clays and the low sand content. For samples taken from a single borehole, undrained shear-strength values can vary by up to a factor of 10; this variation is because of grain size, depositional environment, and post-depositional processes. The maximum undrained shear strength (S_u) appears at the surface, down to −3 m. Su values are 150−180 kPa at the surface, and decrease gradually to 20−40 kPa at −6 m depth. Between 5 and 8 m in mudflat facies, the Su varies between 20 and 40 kPa. Beneath the sand-flat facies, in lagoonal-mud facies, the Su varies between 30 and 50 kPa (Fig. 12).

Compressibility of silty clays

The void ratio (e)–log P curves given in Fig. 13 were obtained on the basis of the conventional oedometer test, done according to ASTM standards. The load-increment ratio is 1.0, and the duration of each load increment is 24 h. Using (e)–log P curves, the pre-consolidation pressure and corresponding overconsolidation-ratio (OCR) values were determined, on the basis of the traditional Cassagrande construction. Some difficulties were encountered in applying the Cassagrande method to samples with low-pronounced yielding curvature. This situation is thought to be because of the silty nature of the samples, low overconsolidated condition, and sample disturbance. As seen in Fig. 14, OCR decreases with depth. OCR values range from 3 to 15; however, the OCR = 2–6 at 5–8 m depth. Below the sand-flat facies, the OCR is less than 2, with an average of 1; this situation is attributed to depositional properties and post-depositional processes. The higher OCR values are because of apparent overconsolidation caused by chemical changes (mainly oxidation) in the weathered-crust zone.

Much research (Nishida 1956; Terzaghi and Peck 1967; Azzouz et al. 1976; Koppula 1981; Herrero 1983; Nakase

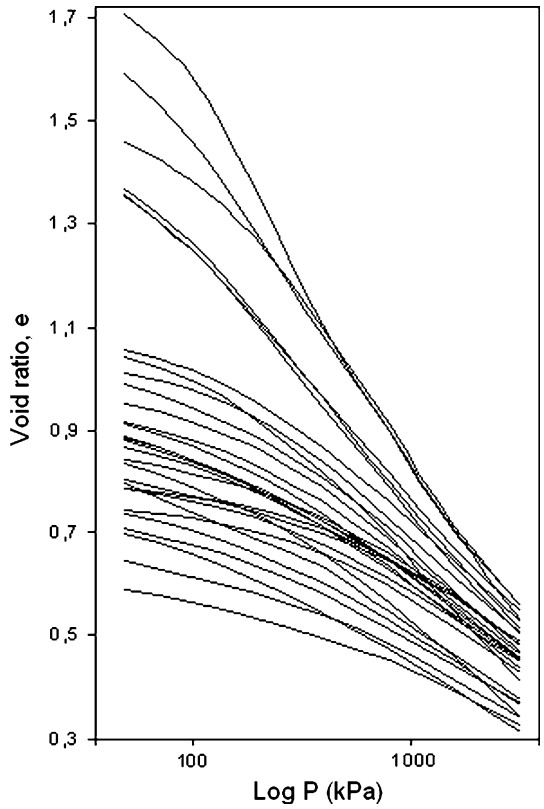

Fig. 13 Void ratio versus log P graphs of soils

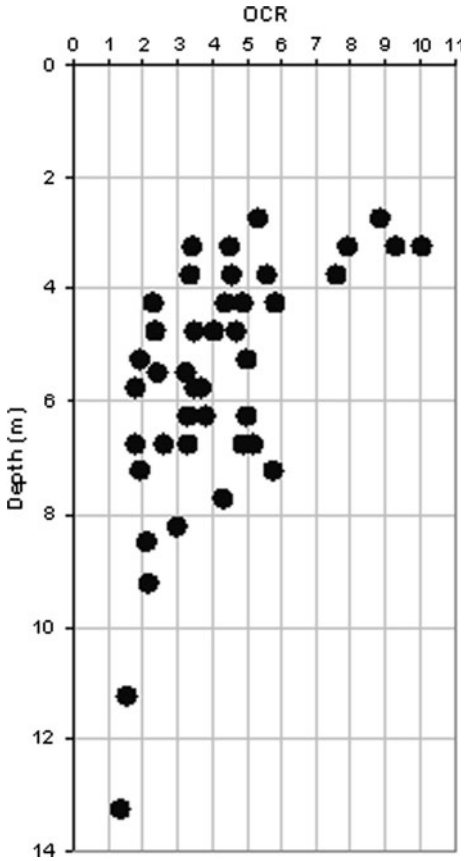

Fig. 14 Variation of overconsolidation ratio with depth

et al. 1988; Yin 1999) has been carried out in order to better understand the relationship between the compression index of clays (C_c) and the basic index properties of soil. However, the literature has given different solutions for different regions or for soils of different origins. Hence, the compression indices of these clays, with some empirical correlations for the lagoonal depositional environment, are given below.

Oedometer test results show that the compression indices for clayey soils of the Bogacay Plain are in the range of 0.25–0.5. The compression indices of the clays were correlated with the moisture content and natural void ratio of the clays to enable quick determination of C_c by use of soil index values. The correlations determined from simple regression analysis are given in Eqs. 1 and 2 respectively. To take into consideration the fabric (structure) and mineralogy of the clays, C_c can be correlated with natural void ratio together with liquid limit, by the relationship given in Eq. 3.

$$C_c = 0.0064 * W_n + 0.106 \quad (R^2 = 0.78) \tag{1}$$

$$C_c = 0.0237 * e_0 + 0.107 \quad (R^2 = 0.79) \tag{2}$$

$$C_c = 0.03 + 0.0001 * LL + 0.01 W_n \quad (R^2 = 0.85) \tag{3}$$

Secondary compression index (C_α) values range from 0.001 to 0.005. Variation of C_α values with depth for BH-29 is shown in Fig. 15. An inverse relationship between C_α and q_c (point resistance of the CPT) is notable.

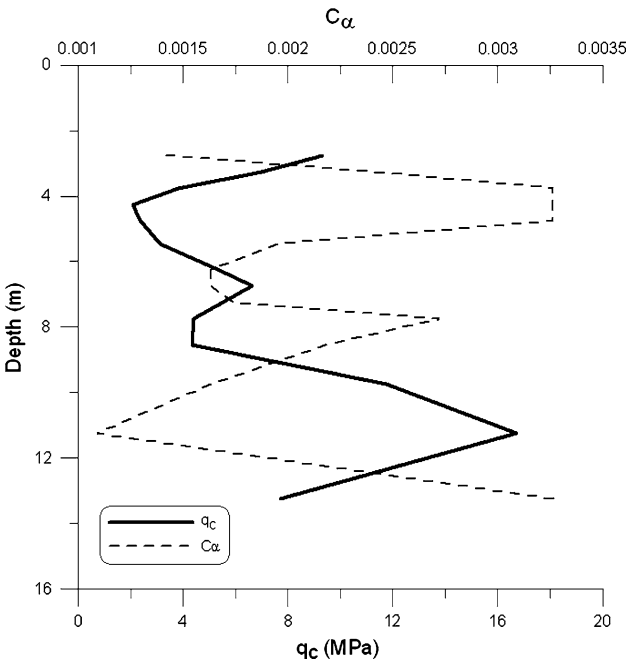

Fig. 15 Variation of secondary compression index with depth

Discussion

Facies identification by means of geotechnical data

One of the main objectives of a site investigation should be to investigate facies variations with depth, and also correlation within given site boundaries. Subsurface lithological mapping by means of facies identification, even though important for geotechnical purposes, is hardly possible using conventional drilling techniques. Any subtle change within the Holocene succession which may be related to structure and, hence, consolidation or strength, can be detected by using continuous probing, for example cone penetration testing. CPT data have been used extensively to assess soil profiles, as reported by Robertson (1990). In addition to soil classification and identification, several

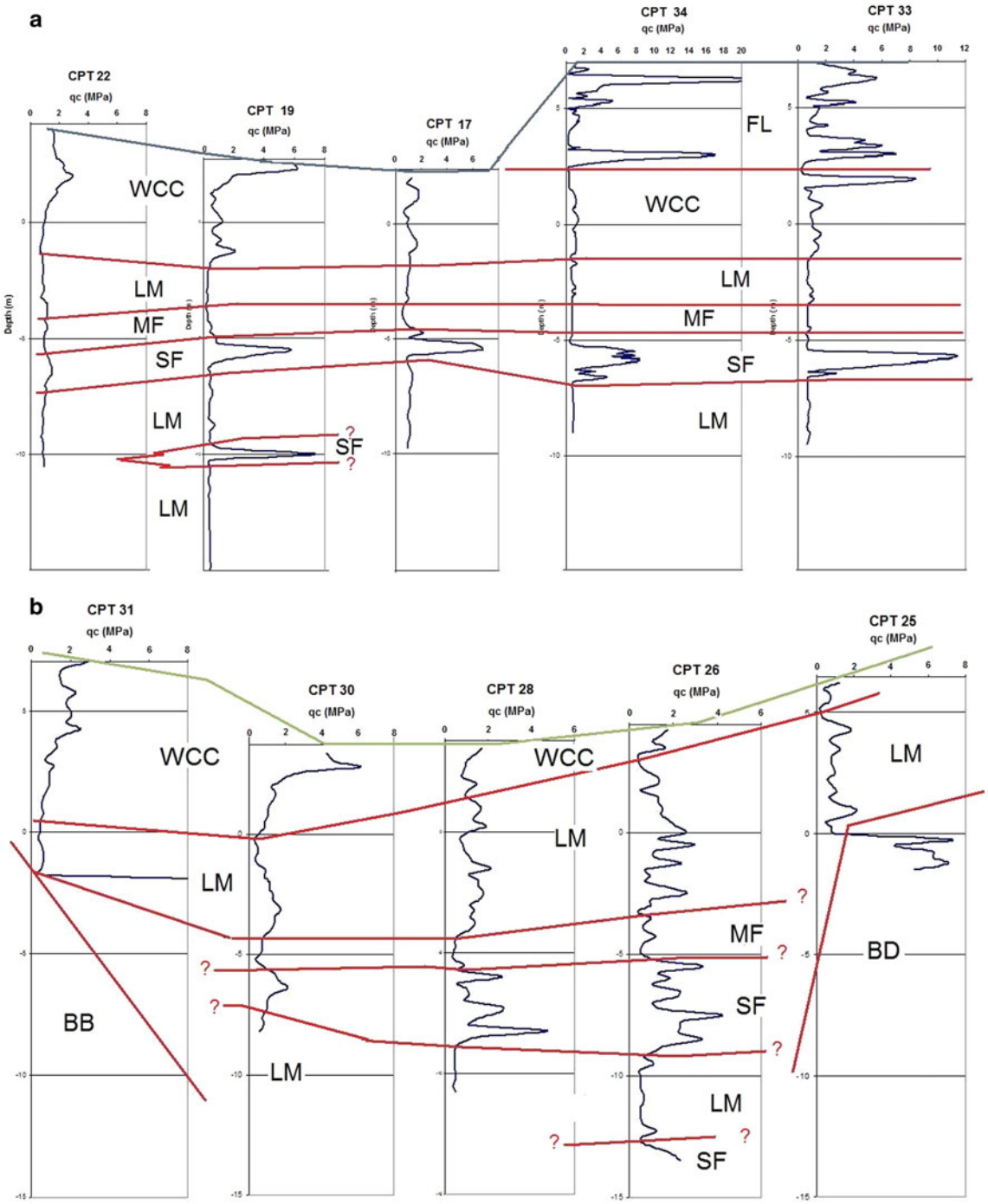

Fig. 16 Facies determination using CPT data

researchers (Gostelow and Lambert 1979; Moran et al. 1989; Amorosi and Marchi 1999; Ricceri et al. 2002; Choi and Kim 2006) have used CPT data in stratigraphic and sedimentological studies.

Sedimentary units can be distinguished in q_c–F_R plots on the basis of grain size (Robertson 1990); however facies identification, which should include depositional environment, may be achieved using core-sample observations. After sufficient core-sample observation and facies identification, and correlation with CPT data, one can extend this to the entire field area through CPT sounding. In Fig. 16, CPT logs are plotted with depth relative to sea level. The graphs clearly show that CPT data are effective in identifying boundaries of soil units. However these boundaries are not sharp but gradual, they can be correlated throughout the area. The sand-flat facies is easily distinguished by its higher q_c and low F_R values. Rhythmic change in grain size within this facies and the presence of sand–silt interlamination are reflected in the fluctuating cone-resistance and friction-ratio values. One other advantage of CPT logs in distinguishing sedimentary facies is overconsolidation or apparent overconsolidation. In Figs. 8 and 16, q_c plots illustrate the general trend that q_c values decrease from the surface down to 6–7 m. Not only is grain size controlling this behaviour but also crust effect because of weathering and leaching. SPT data in Fig. 7 also support this idea, but CPT is more effective regarding measurement scale and having opportunity to detect grain size decrease with F_R data.

Total and differential settlement because of consolidation

Many buildings constructed in the study area suffer from foundation-settlement problems (Fig. 17). Because immediate settlement is accommodated within the structure as it is built, settlement in this context is long-term consolidation settlement. Generally, settlement of buildings occurs shortly (within months) after the beginning of service life, however it may not be evident if there is no substantial tilt. Tilting or differential settlement in the study area occurs for a number of reasons. Local variation in soil compressibility is one reason. Varying environments of deposition and variation in the thickness of compressible soil also contribute to tilting. Structural problems, because of variation in applied loads, and overlapping stresses, because of closely spaced buildings, are other reasons. Some buildings began to tilt after completion, because of the construction of an adjacent building. One other reason for settlement is secondary consolidation. As an example, for the secondary compression index values given in Fig. 15 and the foundation pressures of buildings in the test area, settlement because of secondary compression may reach 10–15% of the total settlement over the service life. In most cases, all of the reasons mentioned above may be valid.

Fig. 17 Leaning structure in the study area

Conclusions

Based on the geological and geotechnical investigations carried out, the following conclusions are drawn:

1. Soils of the Bogacay coastal plain are of lagoonal origin. After sea-level rise during the Holocene, a barrier beach was formed, and the depression behind the barrier served as a depositional environment for mud (silt–clay). During sea-level highstands, tidal, fluvial, and marsh sediments were deposited. All facies typical of the lagoonal environment are present in the geological profile.
2. Geotechnically, mud layers of the central lagoon are the most interesting, and more attention was paid to these soils. Because of a change in grain size and weathered-crust formation, fine-grained soils of the central-lagoon environment show high variability with regard to their geotechnical properties.
3. Sedimentary facies and their boundaries can be detected using CPT data. Before use for this purpose, q_c and F_R values should be calibrated against local soil properties. However, for profiling and facies-boundary detection, SPT and seismic sounding are not as effective as CPT.

4. The compression indices of clays range from 0.25 to 0.55 and correlate relatively well with initial void ratio, liquid limit, and moisture content. The ratio of σ_p/σ'_{vo} (i.e., OCR) varies from 1.4 to 10, and decreases from the surface down to the base of the weathered-crust zone.
5. The undrained shear strength of clays decreases with depth for the first 6 m; this behaviour is because of apparent overconsolidation in the weathered-crust zone.
6. Bearing-capacity problems because of shear failure have not been recorded in the area. However, many buildings constructed in the study area have suffered foundation settlement and tilting. These problems are attributed to variation in soil compressibility and soil thickness, eccentric foundation loading, and overlapping stresses because of closely spaced buildings.

Acknowledgments This study was supported by the Akdeniz University Research Fund (Antalya, Turkey). The author expresses his gratitude to Professor Dr Vedat Doyuran (Middle East Technical University, Ankara-Turkey) for his helpful insights and suggestions throughout the research. I would also like to thank Bulent Cangir and Evren Kilci for their assistance during laboratory and in situ tests.

References

Akay E, Uysal Ş, Poisson A, Cravatte J, Müller C (1985) Antalya Neojen havzasının stratigrafisi. Türkiye Jeoloji Kurultayi Bülteni 28(2):105–121 Ankara

Amorosi A, Marchi N (1999) High-resolution sequence stratigraphy from piezocone tests: an example from the Late Quaternary deposits of the southeastern Po Plain. Sediment Geol 128:67–81

Azzouz AS, Krizek RJ, Corotis RB (1976) Regression analysis of soil compressibility. Soils Found 16(2):19–29

Choi K, Kim JH (2006) Identifying late Quaternary coastal deposits in Kyonggi Bay, Korea, by their geotechnical properties. Geo Mar Lett 26(2):77–89

DSI (1977) Antalya-Bogacay Ovası, Hidrojeolojik Etüt Raporu. D.S.I. 0901-J-1, Ankara

Glover C, Robertson AHF (1998a) Role of regional extension and uplift in the Plio-Pleistocene evolution of the Aksu Basin, SW Turkey. J Geol Soc London 155:365–387

Glover C, Robertson AHF (1998b) Neotectonic intersection of the Aegean and Cyprus tectonic arcs: extensional and strike-slip faulting in the Isparta Angle, SW Turkey. Tectonophysics 298:103–132

Gostelow TP, Lambert JT (1979) Evaluation of Dutch cone soundings as an engineering geological site mapping tool in the Quaternary sediments of the Firth of Forth area. Bull Eng Geol Environ 19(1):216–226

Hamilton EL (1976) Shear-wave velocity versus depth in marine sediments: a review. Geophysics 41:985–996

Herrero OR (1983) Universal compression index equation; closure. J Geotech Eng ASCE 109:755–761

Holzer TL, Bennett MJ, Noce TE, Tinsley JC (2005) Shear-wave velocity of surficial geologic sediments in Northern California: statistical distributions and depth dependence. Earthq Spectra 21(1):161–177

Kayan I (1988) Late Holocene sea level changes on the western Anatolian coast. Paleogeogr Paleoclimatol Paleoecol 68:205–218

Kelletat D (2005) A Holocene sea level curve for the eastern Mediterranean from multiple indicators. Zeitschrift für Geomorphologie 5:1–9

Kneale D, Viles HA (2000) Beach cement: incipient $CaCO_3$-cemented beachrock development in the upper intertidal zone, North Uist, Scotland. Sediment Geol 132:165–170

Koppula SD (1981) Statistical estimation of compression index. Geotech Test J 4(2):68–73

Moran K, Hill PR, Blasco SM (1989) Interpretation of piezocone penetrometer profiles in sediment from the Mackenzie Trough, Canadian Beaufort Sea. J Sediment Petrol 59:88–97

Nakase A, Kamei T, Kusakabe O (1988) Constitute parameters estimated by plasticity index. J Geotech Eng ASCE 114:844–858

Nishida Y (1956) A brief note on the compression index of soil. J Soil Mech Found Div ASCE 82:1–14

Oner A (1995) Patara ve cevresinin jeomorfolojisi. TÜBİTAK YBAG No.106 Proje Raporu

Reinson GE (1992) Transgressive barrier island and estuarine systems. In: Walker RG, James NP (eds) Facies models: response to sea level change. Geological Association of Canada, Stittsville, pp 179–194

Ricceri G, Simonini P, Cola S (2002) Applicability of piezocone and dilatometer to characterize the soils of the Venice Lagoon. Geotech Geol Eng 20:89–121

Robertson PK (1990) Soil classification using the cone penetration test. Can Geotech J 27:151–158

Senel M (1997) 1: 100, 000 Türkiye Jeoloji Haritası, Antalya L11 Paftası. MTA Yayinlari, Ankara

Terzaghi K, Peck RB (1967) Soil mechanics in engineering practice. Wiley, New York

Tezcan D, Okyar M (2006) Seismic stratigraphy of Late Quaternary deposits on the continental shelf of Antalya Bay, northeastern Mediterranean. Cont Shelf Res 26:1595–1616

Uzer AU (2006) Konyaaltı (Antalya) Lagün Killerinin Teorik ve Deneysel İncelenmesi. Unpublished Ph.D. Dissertation, Selcuk Üniversitesi, Fen Bilimleri Enstitüsü, İnşaat Mühendisligi, Konya

Yin JH (1999) Properties and behaviour of Hong Kong marine deposits with different clay contents. Can Geotech J 36:1085–1095